Bistable nematic and smectic anchoring in the liquid crystal octylcyanobiphenyl (8CB) adsorbed on a MoS_2 single crystal

Emmanuelle Lacaze* and Jean Philippe Michel†
GPS, Universités Paris 6 et 7, UMR-CNRS 75-88, Campus Boucicaut, 140 rue de Lourmel, F-75015 Paris, France

Michel Goldmann‡
LURE, Bat 209D, Université Paris Sud, F-91405 Orsay Cedex, France
and OCIIB, Université Paris 5, Free CNRS 20-23, 45 rue des Saints Pères, Paris Cedex 6, France

Marc Gailhanou§
LURE, Bat 209D, Université Paris Sud, F-91405 Orsay Cedex, France

Marc de Boissieu‖
LTPCM INPG, Boîte Postale 75, F-38402 Saint Martin d'Hères, France

Michel Alba¶
Laboratoire Léon Brillouin, UMR CEA-CNRS 12, CEA-Saclay, F-91191 Gif-sur-Yvette Cedex, France
(Received 20 October 2003; published 29 April 2004)

We have studied the anchoring directions imposed on 4-*n*-octyl-4′-cyanobiphenyl (8CB) smectic-*A* and nematic phases by a single crystal of molybdenum disulfide (MoS_2). Combining optical microscopy and x-ray diffraction under grazing incidence we have demonstrated the occurrence of a bistable planar anchoring. A previous study of the two-dimensional (2D) network of adsorbed 8CB molecules under the liquid crystal film allows a direct connection to be made between the interface structure and the anchoring directions, demonstrating that bistability is induced by the presence of two dipolar groups in the skeleton of the 2D network. It is demonstrated that the Landau–de Gennes theory cannot account for the observed anchoring in the nematic phase. The Landau–de Gennes free energy has to be associated with a coupling with both the surface order and the MoS_2 substrate to explain the experimental observations. The hypothesis of a nematic layer under the liquid crystal bulk is postulated in the smectic phase.

DOI: 10.1103/PhysRevE.69.041705 PACS number(s): 61.30.Hn, 61.10.−i, 68.37.Ef

I. INTRODUCTION

It is well known that two major effects compete to impose the anchoring directions of a liquid crystal; first, the substrate roughness whose role has been analyzed by Berreman [1]; second, the interactions between molecules and substrate or between molecules themselves. In the second framework and in the nematic phase case, it is also well known that a knowledge of the configurations of the molecules adsorbed on the substrate is of particular importance in predicting the anchoring directions of the liquid crystal film on a given substrate. In many systems, the adsorbed molecules remain extremely stable, as soon as they interact with the substrate. This stability leads to memory phenomena [2–4], demonstrating the major role of these molecules on the alignment of liquid crystal films. The influence of adsorbed molecules has been demonstrated through numerous second harmonic generation measurements [5–9]. However, it remains to be demonstrated if the underlying substrate loses all influence with respect to the adsorbed molecules.

The major role of adsorbed molecules has been associated with an induced nematic order at the surface. In the case of substrates with mirror symmetry, the Landau–de Gennes theory allows [7,8,10,11] a quantitative prediction of the tilt angle induced by a given adsorbed molecular distribution. However, in the case of high-symmetry surfaces, such as those with threefold symmetry, the surface nematic order parameter is homeotropic despite, in the case of phlogopite mica as a substrate, the presence of adsorbed molecules almost flat on the substrate. In this case, a tristable planar anchoring is observed in bulk. In order to explain the experimental observations [9], a coupling term with the surface order has then been added to the classical Landau–de Gennes theory.

It would now be interesting to determine if such coupling arises only in the case of high-symmetry surfaces. In such a case, the Landau–de Gennes theory could be applied to most surfaces and predictions of anchoring directions would be obtained from the detailed structure of the adsorbed molecules. If a coupling with the surface order occurs more generally, predictions of alignment directions with respect to the adsorbed molecule structures could become more difficult, depending on the coupling characteristics. In this last case however, multistability phenomena could be expected [9].

*Email address: lacaze@gps.jussieu.fr
†Email address: michel@chem.ucla.edu
‡Email address: goldmann@gps.jussieu.fr
§Email address: gailhanou@lure.u-psud.fr
‖Email address: boissieu@ltpcm.inpg.fr
¶Email address: malba@cea.fr

The phenomenon of smectic anchoring remains complicated as compared with nematic anchoring. An experimental work evidenced particularly strong anchoring energies [14] W in a homeotropically anchored smectic phase compared with most of the already measured nematic anchoring energies [12,13] (W of the order of $10^{-3}-10^{-2}$ J m^{-2}). Such values also appear significantly higher than surface tension anisotropies of smectic phases with planar anchoring, nondegenerate [15], or with tilted anchoring [16] (W of the order of 10^{-5} J m^{-2}). The question of the influence of smectic layering on anchoring properties is consequently open. Some theoretical works were recently published, considering homeotropic [17] or close to be planar [18] anchorings.

We have chosen the system of a 4-*n*-octyl-4′-cyanobiphenyl (8CB) film adsorbed on molybdenum disulfide (MoS_2) in order to study these questions. The MoS_2 substrate is flat, avoiding any influence of roughness of the substrate on the anchoring phenomenon. 8CB liquid crystal perfectly wet the MoS_2 substrate leading to formation of homogeneous liquid crystal films. The 8CB/MoS_2 interface has been recently studied directly under the liquid crystal film, allowing an *in situ* connection between the study of adsorbed molecules and the study of anchoring directions, which appears extremely rare in such systems [19]. The connection between polarity of the adsorbed molecules and wetting properties of liquid crystal film can then be confirmed [20]. The 8CB/MoS_2 interface being composed of a very well ordered bidimensional network which does not exhibit any simple symmetry, as the underlying MoS_2 surface exhibits a hexagonal symmetry [21,22], the system also appears particularly well adapted to the study of the respective influences of the underlying substrate and of the adsorbed molecules on the anchoring directions of the liquid crystal, the main problem that we want to address in this paper.

We have studied the anchoring geometry of both phases, smectic *A* and nematic, by optical microscopy (Sec. III A) and by x-ray diffraction in grazing incidence (Sec. III B). In Sec. IV, we connect the determined anchoring directions to the structure of the adsorbed molecules. Results are then discussed, first the question of nematic anchoring and second the question of smectic anchoring.

II. 8CB/MoS_2 INTERFACE

By combining scanning tunneling microcopy (STM) and x-ray diffraction experiments, we have previously determined the microscopic structure of the two-dimensional (2D) monolayer formed by 8CB molecules adsorbed on a MoS_2 substrate, under the 8CB liquid crystal film [21–23].

This 2D monolayer is composed of 2D single crystals, disoriented by 60° with respect to each other, due to the hexagonal symmetry of the underlying substrate. The microscopic structure of each of these crystals, observed by STM, is presented in Fig. 1 which reveals a highly ordered molecular organization, characterized by straight ribbons. Within the ribbons each molecule can be distinguished [see the model on the left of Fig. 1(a)], as well as the respective positions of the cyanobiphenyl group and the alkyl chain within the molecules. From such an image, it can be deduced that the adsorbed molecules are close to flat on the substrate and that, within the ribbons, the molecules adopt a head-to-tail geometry. Figure 1(b) shows the structure as obtained by x-ray diffraction experiments. The network commensurability corresponding to a $c(4\times32)$ superstructure, the ribbons are aligned parallel to the [100] (or [010] and [−1−10]) MoS_2 direction.

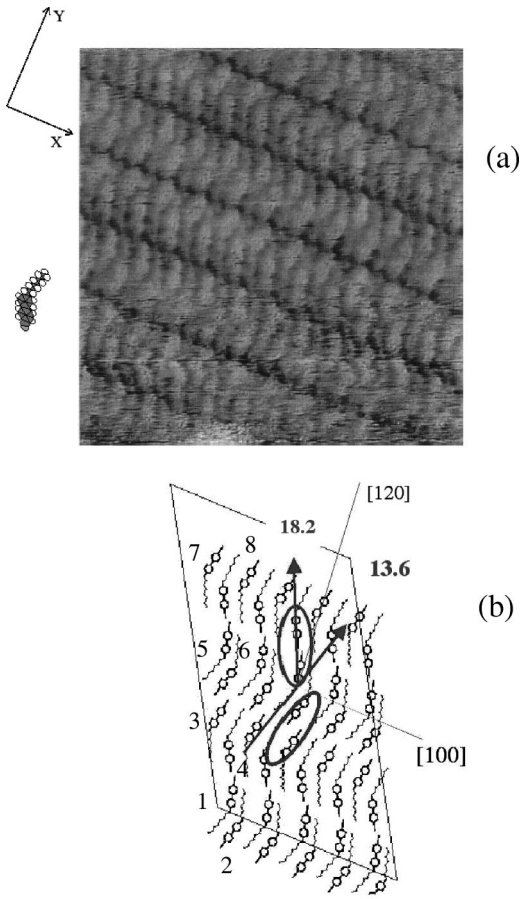

FIG. 1. (a) STM image of the adsorbed 8CB molecules on MoS_2 (14 nm×14 nm; $I_t=0.31$ nA, $V_t=1.6$ V). The molecules on the substrate appear highly 2D oriented, organized in straight ribbons along the X direction. The molecules within the ribbons can be distinguished (see the model on the left) and adopt a head-to-tail geometry. (b) Microscopical structure as determined by x-ray diffraction. The crystallographic cell is formed by the eight molecules labeled 1–8 and corresponds to a $c(4\times32)$ MoS_2 superstructure. The two associated dipolar groups are shown at −13.6° and 18.2° away from the direction perpendicular to the ribbons.

A close inspection of the network reveals that the adsorbed 8CB dipoles are aligned along two main directions [underlined in Fig. 1(b)], at −13.6° and 18.2° away from the direction perpendicular to the ribbons (the [120], the [210], or the [−110] of MoS_2, depending on the considered 2D single crystal).

III. EXPERIMENT

MoS_2 natural single crystals come from Queensland (Australia), supplied by The Ward Company, NY. This lamel-

lar compound can be easily cleaved, thereby revealing a clean surface parallel to the basal planes. The surface is composed of sulfur atoms organized in a hexagonal lattice ($a_{MoS_2}=3.16$ Å as cell parameter), with a mosaicity smaller than 0.02°, as checked by x-ray diffraction. The 8CB is a BDH (BDH-GMBH, Germany) product used without any further purification. The 8CB is smectic *A* at room temperature with the smectic/nematic transition occurring at 33.5 °C and the nematic/isotropic transition around 40 °C. The 8CB film is prepared by spin coating an $8CB/CHCl_3$ solution on the MoS_2 surface, leading to homogeneous films with thicknesses ranging from 0.1 to 1 μm, depending on the 8CB concentration (from 0.1 mol/l to 0.5 mol/l) and the spin coater speed (from 1000 to 6000 rpm). The system is then annealed at 80 °C for 30 min, in order to create ordered 2D crystals at the $8CB/MoS_2$ interface.

Optical microscopy experiments were performed on a polarizing microscope LEICA DMR fitted with a charge-coupled device color camera and a digitizing system for image acquisition. Optical microscopy images were obtained in the reflection mode, due to the opacity of the MoS_2.

X-ray diffraction experiments were performed on the synchrotron beamlines D2AM at ESRF (Grenoble, France) and H10 at LURE (Orsay, France) equipped with four-circle diffractometers. We used a standard configuration: photon energy at 8 keV, horizontally mounted sample oriented by a goniometrical head in order to explore the whole reciprocal space. The full beam spot was delimited close to the sample by a pair of slits leading to a beam size between 50 $\times 500$ μm^2 and 100 $\times 1000$ μm^2, and the intensity was monitored by a diode. The diffracted intensity was scanned parallel to the sample plane by a solid state detector at the smectic momentum transfer $Q_S=0.2$ Å^{-1} of the 8CB molecules. The in-plane and out-of-plane resolutions were of the order of 0.05°.

A. Optical microscopy experiments

Figure 2 presents optical microscopy images between crossed polarizers of the smectic phase [Fig. 2(a)] and of the nematic phase [Fig. 2(b)] of a 0.4 μm thick 8CB film on top of MoS_2.

It shows that the film is composed of domains of different tints, the tint depending on the orientation of the sample with respect to the analyzer direction. The black domains correspond to areas in which anchoring is close to planar and either parallel or perpendicular to the analyzer. Each domain can be extinguished between crossed polarizers for a given orientation of the sample and only 12 discrete orientations of the sample allow the extinction of domains, as shown in Figs. 2(a) and 2(b).

A close inspection of these orientations reveals that six planar anchoring directions are associated with the extinctions, with azimuthal disorientations of 25° (modulo 60°) and 35° (modulo 60°) between these directions. These results can be analyzed as follows.

First the tint of each domain in Figs. 2(a) and 2(b) is identical, the only difference corresponding to the presence of lines in the smectic phase that are not observed in the nematic phase. These lines are interpreted as smectic defects due to antagonistic anchorings between substrate and air [24]. We can conclude from the similarity of the tints and the textures that the smectic *A* and nematic anchorings are identical, as previously observed in case of planar anchoring in several other systems [12,25]. It is then possible to analyze the anchoring directions in both phases, in particular with respect to the substrate crystallographic directions, taking advantage of the periodic character of the smectic phase and using x-ray diffraction experiments (Sec. III B).

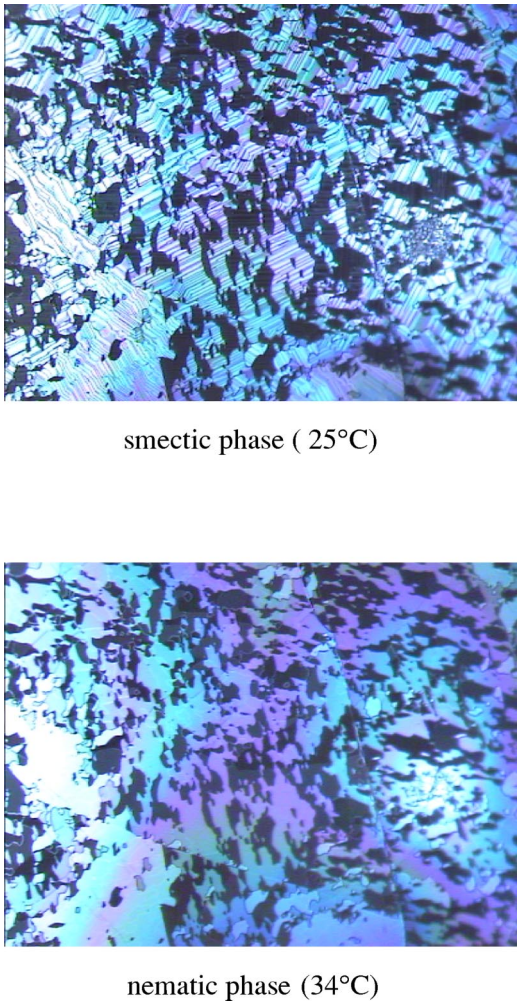

FIG. 2. Optical microscopy images (140 μm$\times$100 μm), between crossed polarizers, of smectic phase ($T=25$ °C) and nematic phase ($T=34$ °C) of a 0.4 μm thick 8CB film on MoS_2.

Second, because each domain can appear colored between crossed polarizers (the color depends on the thickness due to Newton interferences) despite the homeotropic anchoring at the air interface, the anchoring of 8CB on MoS_2 appears close to planar. Such a result is consistent with the observation of molecules lying flat on the substrate in the underlying 8CB 2D network. However, it differs from the results of numerical calculations on a similar system, 8CB on graphite [26], leading to a second layer of molecules already homeotropic with respect to the first layer.

Moreover, the homogeneous tint within each domain, as seen in Fig. 2, shows that the planar anchoring on MoS_2 is

unidirectional within the domains, which have lateral size varying from several tens to several hundreds of micrometers. Only six azimuthal orientations of the planar anchoring are possible for domains of a given sample.

Third, the homogeneity of the liquid crystal color, as observed by optical microscopy, in particular between parallel polarizers, evidences a good homogeneity of the liquid crystal thickness and such a perfect wetting of 8CB on MoS_2, contrary to numerous *n*CB/solid substrate systems [27]. This result can be associated to the nonpolarity of the adsorbed 8CB network, induced by the head-to-tail geometry of the adsorbed molecules within the ribbons (Fig. 1). The difference with the systems 8CB/poly(vinyl cinnamate) (PVCN) or 8CB/quartz, characterized by dewetting associated to polar adsorbed monolayers, confirms the role of polarity on wetting properties of the *n*CB family [20].

B. X-ray diffraction experiments

Due to the homeotropic alignment at the air interface, the smectic planes deform in the bulk to accommodate the two antagonistic anchorings. Consequently, in order to probe the anchoring at the MoS_2 surface, we have to measure the diffracted signal originating from the smectic layers close to MoS_2. This corresponds to a small amount of matter buried below the liquid crystal bulk and requires the use of synchrotron sources. In order to specifically detect the perpendicularly anchored smectic layers associated with planar anchoring, we work in grazing incidence geometry.

In such a geometry the incident (and exit) tilt angle is fixed close to the MoS_2 critical angle [$\theta_C(MoS_2)=0.344°$ at 8 keV], in order to only slightly penetrate the bulk MoS_2, but higher than the 8CB critical angle [$\theta_C(8CB)=0.172°$ at 8 keV) in order to penetrate the bulk liquid crystal and indeed probe the smectic layers close to MoS_2. The incidence angle is fixed at $\theta_i=0.3°$ and the lateral angular position of the detector is fixed at $2\theta=2\theta_S\cos(\theta_i)$, $\theta_S=1.4°$ corresponding to the smectic layer period for 8 keV photons, associated with a smectic wave vector [28] of $Q_S=0.2$ Å^{-1}. In such a geometry, the diffracting layers are almost perpendicular to the substrate surface and disoriented with respect to the incident beam by an angle denoted by ϕ. Keeping the incident beam and the detector fixed, the sample is rotated (the ϕ value is varied) over 180° in order to detect the smectic Bragg peaks corresponding to all perpendicularly anchored smectic layers. Once the MoS_2 Bragg peaks have been measured, the azimuthal anchoring orientation can be determined with respect to the main crystallographic directions of MoS_2.

A typical result can be seen in Fig. 3, which shows the diffracted intensity versus the sample orientation over 180°. In this generic scan, only five peaks of different intensities are detected.

The detection of intense peaks in grazing incidence geometry demonstrates that indeed the anchoring of the smectic phase is planar on MoS_2 as well as the anchoring of the nematic phase. This scan reveals a very limited number of anchoring directions on a given sample. In the case of Fig. 3, five directions are detected at $-41°\pm0.5$, $-76°\pm0.5$, $-101°\pm0.5$, $-136°\pm0.5$, $-161°\pm0.5$. These values are disoriented at 35° or 25° away from each other. These orientations are then compatible with the sample orientations, leading to the extinction of domains in optical microscopy between crossed polarizers (Sec. III A). This shows that each Bragg peak of Fig. 3 corresponds to one kind of domain orientation, observed in optical microscopy, confirming in particular the planar unidirectional anchoring within a given domain.

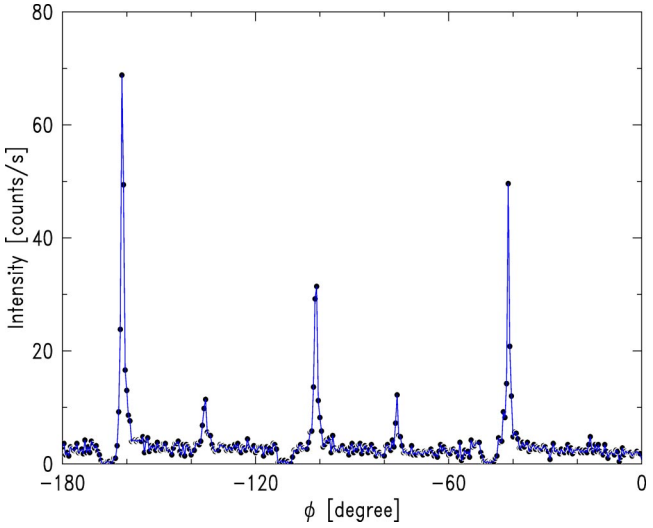

FIG. 3. X-ray diffraction intensity variation during the rotation over 180° of a 0.4 μm thick 8CB film on top of MoS_2. Five peaks are measured at $-41°\pm0.5$; $-76°\pm0.5$; $-101°\pm0.5$; $-136°\pm0.5$, $-161°\pm0.5$. The pronounced dips at $-165.5°$, $-111°$, and $-45.5°$ correspond to the furnace tungsten pillars passing either in the direct beam or in front of the detector.

It is also possible to determine the azimuthal orientations with respect to the MoS_2 crystallographic directions in the case of a sample previously oriented with respect to the substrate. The θ_S value then has to be subtracted from the different ϕ values, leading to Bragg peaks in Fig. 3 associated with smectic layers at $-42.4°\pm0.5$, $-77.4°\pm0.5$, $-102.4°\pm0.5$, $-137.4°\pm0.5$, $-162.4°\pm0.5$ away from the MoS_2 [100] direction. If we now combine our measurements performed on 12 different samples, we obtain the following result: on a given sample, only six planar anchoring directions exist at $\pm17.5°\pm0.4$ (modulo 60°) away from the MoS_2 [100] direction.

The differences of intensity of the peaks in Fig. 3 demonstrate that the proportions of the six domains are different on the measured area. This has to be related to the large size of the domains, between several tens and several hundreds of micrometers as observed by optical microscopy, which is therefore of the same order as the beam size—between 500 and 1000 μm. Figure 4 shows an enlarged view of a Bragg peak of Fig 3, associated to smectic layers at 17.5° away from the MoS_2 [−1−10] direction. The measured mosaicity of the anchored smectic layers is $\Delta\phi=0.39°$. This leads in Å^{-1} to $\Delta q=q\Delta\phi=1.4\times10^{-3}$ Å^{-1} which is of the same order as the mosaicity of a similar smectic compound oriented by an average magnetic field of 1 T [29]. This result demonstrates how a crystalline substrate such as MoS_2 can strictly orient smectic layers within a given domain, in particular with respect to gratings on glass or silicon, on which

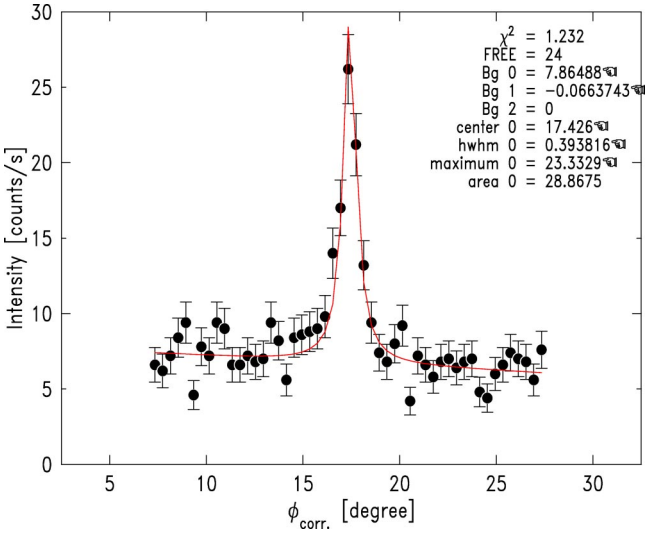

FIG. 4. X-ray diffraction intensity on a given Bragg peak showing the anchored smectic layers orientation and mosaicity. It corresponds to the peak of Fig. 3 at −101° offset by 120°, corrected by the $\theta_S = 1.4°$ angle and the grazing incidence geometry. The observed 0.39° mosaicity corresponds to a value of 1.4×10^{-3} Å^{-1} in wave-vector units.

the mosaicity of perpendicularly anchored smectic layers is higher by one to two orders of magnitude [30].

IV. RELATIONSHIP BETWEEN THE ANCHORING DIRECTION AND THE 8CB/MoS_2 INTERFACE STRUCTURE

We now turn the question of the origin of the observed anchoring, in particular the origin of the measured anchoring directions, at ±17.5° (modulo 60°) away from the MoS_2 [100] direction. The observed degeneracy is clearly related to the hexagonal symmetry of the MoS_2 substrate. More precisely it is related to the presence in the underlying 2D 8CB network of 2D single crystals, disoriented by 60° from each other. Indeed, as shown by STM and x-ray diffraction [21], these 2D single crystals are definitely larger than 1 μm, which strongly suggests that they impose the unidirectional anchoring of the 8CB bulk film on top. In other words, for a given orientation of the ribbons characterizing the 8CB/MoS_2 interface (parallel to the [100], [010] or [−1−10] MoS_2 directions), the smectic (and nematic) director is oriented at ±17.5° away from the direction perpendicular to the ribbons (the [120], [210], or [−110] MoS_2 direction), as shown schematically in Fig. 5.

A. Nematic anchoring

Let now discuss about the evolution predicted by a Landau–de Gennes theory within the frame of a single 2D crystal characterizing the interface 8CB/MoS_2. In the case of an interface having a planar uniaxial nematic order parameter, the nematic order parameter orientation does not vary from the surface to the bulk, remaining parallel to the interface. The order parameter value varies only towards its bulk value S_b which is of the order of 0.6 in case of 8CB in the

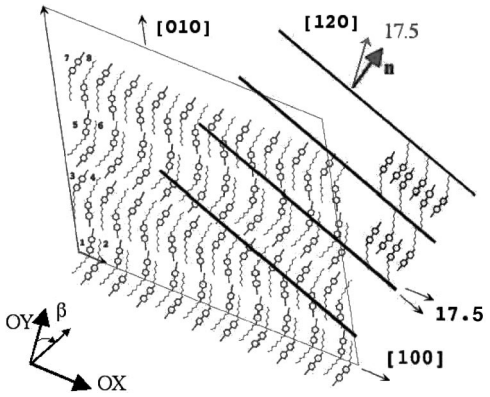

FIG. 5. Design showing the adopted geometry of perpendicularly anchored smectic layers with respect to an underlying 2D adsorbed single crystal. The axes OX (parallel to the ribbons) and OY (perpendicular to the ribbons) used for the calculation of the surface nematic order parameter are indicated, as well as β, the calculated in-plane nematic director disorientation with respect to the (OY) axis.

nematic phase [31]. However, in the case of low-symmetry surface networks such as the one of a 2D single crystal of the 8CB/MoS_2 interface, the surface order parameter is not uniaxial. The observed disorientation of the bulk order parameter could then be connected to the biaxiality of the surface order parameter and to its evolution towards the uniaxial bulk order parameter, as the bulk pretilt can be associated with the surface biaxiality out of the substrate plane, as in the case of 5CB adsorbed on rubbed polyimide [7].

The knowledge of the respective orientations of the eight adsorbed molecules in the 8CB/MoS_2 network cell allows us to calculate the surface nematic order parameter, following the usual definition [32] and taking into account the molecular orientation as imposed by the molecular dipole. The nematic tensor is defined as following:

$$Q_{ij} = \left\langle \frac{3a_i a_j - \delta_{ij}}{2} \right\rangle, \tag{1}$$

$\vec{a}$ being the molecular dipole direction.

The frame in which this tensor can be diagonalized gives the nematic director direction, as well as the two order parameters S and P such that

$$\vec{Q} = \begin{pmatrix} Q_{x'x'} & 0 & 0 \\ 0 & Q_{y'y'} & 0 \\ 0 & 0 & -1/2 \end{pmatrix} = \begin{pmatrix} \frac{-S+P}{2} & 0 & 0 \\ 0 & S & 0 \\ 0 & 0 & \frac{-S-P}{2} \end{pmatrix}$$

in the case of a planar anchoring and a nematic director oriented along the y′ axis.

In the axis associated with the direction parallel (OX), perpendicular (OY) to the ribbons and normal to the surface (OZ) (see Fig. 5), the different values of the surface nematic tensor are $Q_{yyo} = 0.88$, $Q_{zzo} = -0.5$, and $Q_{xyo} = 0.052$ with $Q_{xxo} = -Q_{yyo} - Q_{zzo} = 0.38$, if we consider the average orientation of the adsorbed dipoles, the subscript o correspond-

ing to surface parameters. The diagonalization of such a tensor gives the value of the cosine of the angle β_o of the surface nematic director with respect to the (OY) axis (see Fig. 5):

$$\cos(\beta_o)=1/\left[\sqrt{1+\frac{\left[Q_{yyo}+\frac{Q_{zzo}}{2}-\sqrt{Q_{xyo}^2+\left(Q_{yyo}+\frac{Q_{zzo}}{2}\right)^2}\right]^2}{Q_{xyo}^2}}\right] \tag{2}$$

leading to the value $\beta_o=2.36°$. In the 2.36° tilted frame, the diagonalized tensor corresponds to an order parameter $S_o=0.882$ and to a biaxial term $P_o=0.118$. The surface order parameter appears higher than the bulk one, as in the case of a similar system, 8CB/graphite [33]. The surface biaxiality is small, as well as the in-plane tilt with respect to the direction perpendicular to the ribbons (OY).

It is now possible to estimate the evolution of the nematic order parameter towards the bulk, using the Landau–de Gennes free energy density [10,11]

$$f=\tfrac{1}{2}[A_q(Q_{ij}-Q_{ijb})^2+L_1Q'_{ij}Q'_{ij}+L_2Q'_{iz}Q'_{iz}] \tag{3}$$

with A_q, L_1, and L_2 being phenomenological constants [7,8,10] and the subscript $_b$ corresponding to bulk parameters associated with the bulk values $S_b=0.6$ and $P_b=0$. The values $A_q/L_2=0.01\ \mathrm{nm}^{-2}$ [8] and $L_1/L_2=2/5$ [8,18,34] can be used, the case of 5CB being adapted to 8CB.

The evolution of the different terms of the nematic tensor can be calculated by solving the Euler-Lagrange equations. One obtains

$$Q_{zz}(z)=Q_{zzb}+(Q_{zzo}-Q_{zzb})e^{-z[3A_q/(3L_1+2L_2)]^{1/2}}, \tag{4}$$

$$Q_{xy}(z)=Q_{xyb}+(Q_{xyo}-Q_{xyb})e^{-z(A_q/L_1)^{1/2}}, \tag{5}$$

$$Q_{yy}(z)=Q_{yyb}+\left(Q_{yyo}-Q_{yyb}+\frac{Q_{zzo}-Q_{zzb}}{2}\right)e^{-z(A_q/L_1)^{1/2}} -\left(\frac{Q_{zzo}-Q_{zzb}}{2}\right)e^{-z[3A_q/(3L_1+2L_2)]^{1/2}}. \tag{6}$$

The values of Q_{zzb}, Q_{xyb}, and Q_{yyb} can be deduced from the bulk values $S_b=0.6$ and $P_b=0$ and from the minimization of the free energy $F=\int f dz$ with respect to Q_{yyb}. This minimization leads to a fourth-order polynomial which can be solved numerically, leading to the following values: $Q_{zzb}=-0.3$, $Q_{xyb}=0.028$, and $Q_{yyb}=0.599$.

The disorientation of the bulk nematic director can finally be calculated, using the limiting value of $\beta(z)$ such that

$$\cos(\beta_b)=1/\left[\sqrt{1+\frac{\left[Q_{yyb}+\frac{Q_{zzb}}{2}-\sqrt{Q_{xyb}^2+\left(Q_{yyb}+\frac{Q_{zzb}}{2}\right)^2}\right]^2}{Q_{xyb}^2}}\right], \tag{7}$$

$\beta_b=1.83°$.

The evolution of the in-plane tilt with respect to the (OY) axis remains small as in the case of 5CB on rubbed polyimide, with a different geometry but also a weak biaxiality. β_b is then clearly different from the experimental value, 17.5°. This demonstrates that in the $8\mathrm{CB}/\mathrm{MoS}_2$ system, the Landau–de Gennes theory cannot describe the evolution of the nematic order parameter, contrary to the case of 5CB on rubbed polyimide.

As for high-symmetry interfaces (5CB on phlogopite mica) [9], a coupling with the adsorbed molecules needs to be introduced in order to interpret the results. Indeed, instead of being imposed by the surface nematic order parameter and therefore being close to the direction perpendicular to the ribbons, the bulk nematic director is oriented at $\pm 17.5°$ away from this direction. The value 17.5° appears close to the orientations of the two dipolar groups forming the skeleton of the $8\mathrm{CB}/\mathrm{MoS}_2$ network, at $-13.6°$ and 18.2° away from the direction perpendicular to the ribbons [see Fig. 1(b)]. A coupling with the surface order associated with the molecular dipoles can then be postulated in order to explain the observations. The surface order appears coupled to the nematic order parameter as a surface order with a mirror symmetry would be, favoring one of the two corresponding directions, each being associated with a dipolar group. This finally leads to a bistable anchoring, the two corresponding directions being disoriented from each other by $2\times 17.5=35°$.

In the case of a high-symmetry interface (5CB/phlogopite mica), no preferred orientation is predicted with the Landau–de Gennes theory, due to the homeotropic surface nematic order parameter. So only a weak coupling with the surface order can impose particular planar anchoring directions. This is not true in case of a low-symmetry interface such as $8CB/MoS_2$. It means that, in order to impose anchoring directions different from the one associated to a Landau–de Gennes evolution, the coupling with the surface order parameter needs to be strong. Such a strong coupling could be related to the particularly well-defined interfacial structure, essentially without any disorder.

However, if the two dipolar group orientations are close to the director orientations, they are not strictly equal. In other words, the observed director orientations appear symmetric with respect to the direction perpendicular to the ribbons, whereas, with two different orientations for the two dipolar groups at $-13.6°$ and $18.2°$, the adsorbed structure does not present such a symmetry. This difference suggests that the high-symmetry underlying substrate also plays a non-negligible role on the selection of the anchoring directions, in addition to the minimization of the Landau–de Gennes free energy and the coupling with the surface order. The role of the substrate on the anchoring could be, however, larger in the $8CB/MoS_2$ system than in many other systems. Indeed, adsorbed 8CB molecules on MoS_2 appear flat such that the distance between the substrate and the second 8CB layer is still small, allowing non-negligible electrostatic interactions to take place. The observation of such a role for MoS_2 is consistent with the recent demonstration of a strong interaction between the substrate and the adsorbed molecules in the same system, likely associated with electrostatic interactions [23].

B. Smectic anchoring

The anchoring geometries of nematic and smectic-*A* phases are similar, and then both phases are connected to the coupling between the adsorbed dipoles and the director. In most previously studied cases of smectic anchoring that also present similar anchoring of smectic-*A* and nematic phases, the adsorbed structure was not accurately determined.

In the $8CB/MoS_2$ system, we can now assess that, if the connection between the orientation of the interface and the orientation of both phases can be understood, this is obviously not the case of a connection between the structure of the interface and the structure of the smectic layers. Indeed, the ribbon period is equal to 25 Å, considerably smaller than the smectic layers period of 31.6 Å. However the smectic phase appears strongly enough anchored, as demonstrated by the optical microscopy observations, so that the anchoring on MoS_2 remains planar and antagonistic with respect to the homeotropic anchoring at the other interface (8CB/air) for thicknesses as small as 0.09 μm.

A possible hypothesis to explain such a result consists in assuming the presence of a nematic layer between the $8CB/MoS_2$ interface and the smectic bulk in which smectic layers would be melted. Indeed a rough calculation, considering the number of edge dislocations necessary to accommodate the smectic layers and the ribbons (one dislocation over six ribbons), associated with the cost of an isolated dislocation (of the order of K [35], $K=7\times10^{-12}$ J m^{-1} being the 8CB curvature modulus [36]) leads to a distortion energy of 5.5×10^{-4} J m^{-2} for smectic layers directly connected to the ribbons.

This value can be compared to a rough calculation of the energy of a 1 nm thick (δ) nematic layer at 25 °C, considering that the nematic layer replaces a smectic layer of order parameter equal to the smectic bulk order parameter: $F=[a/2\Psi^2(T_0-T)-b/4\Psi^4]\delta=\delta(a^2(T-T_0)^2)/4b$, $F=5.69\times10^{-4}$ J m^{-2}. Ψ is the smectic order parameter, T_0 the smectic/nematic transition temperature ($T_0=33.5$ °C), a and b the second- and fourth-order coefficients in the de Gennes free energy versus Ψ. The a^2/b ratio is obtained from the experimental determination of the heat capacity of 8CB [37] ($a^2/b=3.15\times10^4$ J K^{-2}m^{-3}).

Since both energies are similar, the hypothesis of a thin nematic layer between $8CB/MoS_2$ interface and smectic bulk appears acceptable, in particular if we consider that the smectic distortions have been probably underestimated, regarding for example the disorientation of the ribbons with respect to the smectic layers. A nematic layer would be in particular clearly favored in the presence of a nematic surface potential, whose existence has been recently postulated [17] in order to interpret experimental results on 10CB adsorbed on a silane substrate [38] with homeotropic anchoring.

The existence of such a nematic layer would be particularly natural in case of planar or tilted anchorings on substrates, either structurally disordered, or particularly well ordered with no matching between the interface order and the smectic order. However, the hypothesis of a nematic layer close to the substrate differs from the theoretical interpretation of experimental observations on the system 5CB/rubbed polyimide [18], in which perfect surface smectic order is obtained with an anchoring close to be planar. The existence of a nematic layer would then depend on the substrate nature. The presence of such a nematic layer could be consistent with high orientational anchoring energies but should at least impose a low positional anchoring energy. This last parameter has been measured for the system butiloxy-benzylideneoctylaniline (4*O*.8)/silicium oxide (SiO) associated with a planar anchoring [39], indeed leading to a low value of the positional anchoring energy, of the order of 10^{-8} J m^{-2}, also associated with a very low surface smectic order value ψ_s of the order of 10^{-5}.

V. CONCLUSION

By combining optical microscopy and x-ray diffraction in grazing incidence, we have determined the anchoring directions in both nematic and smectic-*A* phases of 8CB on a well ordered interface formed by the 2D 8CB network adsorbed on MoS_2.

The comparison of these results with the structure of the 2D 8CB network demonstrates that, on such an ordered interface, the bulk director orientation is not only determined through the minimization of the Landau–de Gennes free energy. A coupling with the 2D surface order and with the

underlying substrate through long range interactions must be taken into account as well. The combination of these three terms finally leads to a bistable anchoring. Such a bistability is directly induced by the adsorbed 8CB structure and could be considerably less influenced by memory effects than most of other multistable anchorings.

In order to interpret the observed similar anchoring directions of the smectic-*A* and nematic phases, the existence of a thin nematic layer between the 2D network and the smectic bulk has been postulated and appears consistent with the high energy of smectic layers directly connected to a highly organized interface.

ACKNOWLEDGMENTS

We gratefully acknowledge R. Lacaze for useful discussions and Professor C. M. Knobler for careful reading of the manuscript.

[1] D.W. Berreman, Phys. Rev. Lett. **28**, 1683 (1972).
[2] N.A. Clark, Phys. Rev. Lett. **55**, 292 (1985).
[3] M. Nobili, R. Barberi, and G. Durand, J. Phys. II **5**, 531 (1995).
[4] R. Barberi, I. Dozov, M. Giocondo, M. Iovane, P. Martinot-Lagarde, D. Stoenescu, S. Tonchev, and L.V. Tsonev, Eur. Phys. J. **6**, 83 (1998).
[5] D. Johannsmann, H. Zhou, P. Sonderkaer, H. Wierenga, B.O. Myrvold, and Y.R. Shen, Phys. Rev. E **48**, 1889 (1993).
[6] B. Jerome, J. O'Brien, Y. Ouchi, C. Stanners, and Y.R. Shen, Phys. Rev. Lett. **71**, 758 (1993).
[7] X. Zhuang, L. Marrucci, and Y.R. Shen, Phys. Rev. Lett. **73**, 1513 (1994).
[8] B. Jerome, J. Phys.: Condens. Matter **6**, A269 (1994).
[9] P.C. Schuddeboom and B. Jerome, Phys. Rev. E **56**, 4294 (1997).
[10] P.G. de Gennes, Mol. Cryst. Liq. Cryst. **12**, 193 (1971).
[11] E. B. Priestley, P. J. Wojtowicz, and P. Sheng, *Introduction to Liquid Crystals* (Plenum Press, New York, 1975).
[12] B. Jerome, Rep. Prog. Phys. **54**, 391 (1991).
[13] M. Vilfan, A. Mertelj, and M. Copic, Phys. Rev. E **65**, 041712 (2002).
[14] Z. Li and O.D. Lavrentovich, Phys. Rev. Lett. **73**, 280 (1994).
[15] A. Hochbaum and M.M. Labes, J. Appl. Phys. **53**, 2998 (1981).
[16] C. Blanc, Phys. Rev. E **64**, 011702 (2001).
[17] I. Lelidis and P. Galatola, Phys. Rev. E **66**, 010701 (2002).
[18] T. Qian, X. Zhuang, and Y.R. Shen, Phys. Rev. E **59**, 1873 (1999).
[19] K. Kocevar and I. Musevic, Liq. Cryst. **28**, 599 (2001).
[20] I.D. Olenik, K. Kocevar, I. Musevic, and T. Rasing, Eur. Phys. J. E **11**, 169 (2003).
[21] E. Lacaze, M. Alba, M. Goldmann, J.P. Michel, and F. Rieutord, Appl. Surf. Sci. **175**, 337 (2001).
[22] J.P. Michel, E. Lacaze, M. Alba, and M. Goldmann, Surf. Sci. **507**, 374 (2002).
[23] E. Lacaze, M. Alba, M. Goldmann, J. P. Michel, and F. Rieutord, Eur. Phys. J. B (to be published).
[24] J. P. Michel, E. Lacaze, M. Alba, M. de Boissieu, M. Gailhanou, and M. Goldmann, Phys. Rev. E (to be published).
[25] P. Hubert, H. Dreyfus, D. Guillon, and Y. Galerne, J. Phys. II **5**, 1371 (1995).
[26] V. Palermo, F. Biscarini, and C. Zannoni, Phys. Rev. E **57**, 2519 (1998).
[27] M. Bardova and R.H. Tredgold, Mol. Cryst. Liq. Cryst. **355**, 289 (2001).
[28] D. Davidov, C.R. Safinya, M. Kaplan, S.S. Dana, R. Schaetzing, R.J. Birgeneau, and J.D. Litster, Phys. Rev. B **19**, 1657 (1979).
[29] A. Primak, M. Fisch, and S. Kumar, Phys. Rev. Lett. **88**, 035701 (2002).
[30] E. Smela and L.J. Martinez-Miranda, J. Appl. Phys. **73**, 3299 (1993).
[31] P.L. Sherrel and D.A. Crellin, J. Phys. (Paris), Colloq. **40**, c3 (1979).
[32] P. G. de Gennes and J. Prost, *The Physics of Liquid Crystals* (Oxford Science, Oxford, 1993).
[33] K. Weiss, C. Woll, and D. Johannsmann, J. Chem. Phys. **113**, 11 297 (2000).
[34] N.V. Madhusudana and R. Pratibha, Mol. Cryst. Liq. Cryst. **89**, 249 (1982).
[35] M. Kleman, *Introduction to Liquid Crystals* (Les Editions de Physique, Paris, 1977).
[36] M.J. Bradshaw and E.P. Raynes, J. Phys. (Paris) **46**, 1513 (1985).
[37] J. Thoen, H. Marynissen, and W. Van Dael, Phys. Rev. A **26**, 2886 (1982).
[38] T. Moses, Phys. Rev. E **64**, 010702 (2001).
[39] M. Cagnon and G. Durand, Phys. Rev. Lett. **70**, 2742 (1993).